*Journal of Machine Engineering, Vol. 15, No.1, 2015*

*machine tool, mutlibody model,*
*component coupling,*
*harmonic analysis*

Jindrich SUSEN[1*]
Matej SULITKA[1]
Jaroslav SINDLER[1]
Miroslav JANOTA[1]

# COMPARISON OF TWO MODEL COUPLING METHODS FOR JOINT IDENTIFICATION

An experimental identification of joint dynamic properties requires accurate models of the joined bodies and an appropriate model coupling method. The bodies to be coupled can be described by their mass, stiffness and damping matrices (M, K, C) or by receptance matrices. Each approach has its advantages and disadvantages. The receptance matrix method requires a high number of measurements. However the measured data can be used directly and no model identification is needed. The experimental identification of the M, K, C matrices feasible for creating precise coupled models is difficult. Therefore, an approach based on a verified FE model can be employed. The two methods of model identification and coupling are discussed using a case study of two bolted beams. Several ways of the receptance matrices measurement simplification and their influence on the accuracy of the results are studied. The effect of noise, measured FRF peak accuracy and data filtering on the resulting coupled receptance matrix is studied as well. The results obtained by the receptance matrix method are compared to the results obtained by the method of coupling the verified FE models. It has been found that the method based on coupling the verified M, K, C matrices proves to be a more reliable approach, which will allow a more precise joint dynamic model identification in the next step.

## 1. INTRODUCTION

High speed and accuracy requirements make machine tool designers carefully consider dynamic behavior of the machines as chatter instability and noise can result from machine's poor dynamic properties. A commonly used tool in dynamics optimization is the finite element method (FEM) which can predict mode shapes, natural frequencies and frequency response functions (FRF). The problem is that there is no reliable way of predicting the machine damping due to unknown damping properties of joints between the machine tool parts. This makes prediction of amplitudes in FRFs and identification of the critical mode shapes difficult.

[1] Czech Technical University, Faculty of mechanical Engineering, RCMT, Prague, Czech Republic
[*] E-mail: J.Susen@rcmt.cvut.cz

There are several sources of damping in machine tool: structural parts, linear guides, bearings, stationary joints etc. While damping in structural parts can be often modeled as proportional, damping in joints, bearings and linear guides (with rolling elements, hydrostatic, sliding) is more complex.

A detailed summary of research of the joint properties can be found in [1]. There was active research concerned with the damping capacity of joints in 1960s and 1970s. Some expressions for the damping capacity have been proposed, however their general applicability has not been verified.

In [2] a research focusing on bolted joint identification using FE models of the coupled parts and a set of springs representing the interface is presented. However, the disadvantage of this approach is that the set of discrete springs does not allow for capturing the interface complex behavior, including the translational and torsional cross-effects. Therefore, a modified approach is proposed in this paper considering the interface representation by the mass, damping and stiffness matrices $\boldsymbol{M_I}$, $\boldsymbol{C_I}$, $\boldsymbol{K_I}$ or by the receptance matrix $\boldsymbol{H_I}$. Parts to be joined can be described by either their receptance matrices $\boldsymbol{H_{S1}}$ and $\boldsymbol{H_{S2}}$ measured directly on the specimens (before they are bolted together) or by the mass, damping and stiffness matrices $\boldsymbol{M_{Si}}$, $\boldsymbol{C_{Si}}$, $\boldsymbol{K_{Si}}$.

Accurate models of the coupled parts represent the main prerequisite for the joint identification method to deliver relevant results. Each of the approaches mentioned above for describing the part models has some advantages and drawbacks. Therefore, the main aim of this paper is to evaluate both approaches with respect to their robustness and precision.

In the first section a general framework for the joint properties identification is introduced, followed by the description of the interface and parts representation methods and their discussion. A case study of a two beam structure is considered and used for the model verification.

## 2. GENERAL FRAMEWORK FOR THE JOINT PROPERTIES IDENTIFICATION

The task on joint properties identification is based on employing the coupled system mathematical model consisting from the models of flexible bodies joined with the interface model. As mentioned above, either receptance matrix representation or FE models of the parts to be coupled are considered. Similarly, the interface is represented by its mass, damping and stiffness matrices $\boldsymbol{M_I}$, $\boldsymbol{C_I}$, $\boldsymbol{K_I}$., or by the receptance matrix $\boldsymbol{H_I}$.

Strategy to mathematical coupling the models and joint properties identification is presented considering the case of $\boldsymbol{M}$, $\boldsymbol{C}$, $\boldsymbol{K}$ matrices. The first step in the identification process is coupling of the system matrices of two bodies $\boldsymbol{M_{Si}}$, $\boldsymbol{C_{Si}}$, $\boldsymbol{K_{Si}}$ and the interface matrices $\boldsymbol{M_I}$, $\boldsymbol{C_I}$, $\boldsymbol{K_I}$. This is done using the coupling equations [3] in a way similar to global matrix assembly in FE software. The equations of motion of the coupled subsystem can be written as:

$$\boldsymbol{M}\ddot{x} + \boldsymbol{C}\dot{x} + \boldsymbol{K}x = f + g \qquad (1)$$

The matrices $\boldsymbol{M}$, $\boldsymbol{C}$, $\boldsymbol{K}$ are diagonal matrices containing the subsystem matrices. Vectors $f$ and $g$ are column vectors containing the subsystem internal and external force vectors respectively.

$$\begin{aligned} \boldsymbol{M} &= diag(M_{S1}, M_{S2}, M_I) \\ \boldsymbol{C} &= diag(C_{S1}, C_{S2}, C_I) \\ \boldsymbol{K} &= diag(K_{S1}, K_{S2}, K_I) \end{aligned} \qquad x = \begin{bmatrix} x_{S1} \\ x_{S2} \\ x_I \end{bmatrix} f = \begin{bmatrix} f_{S1} \\ f_{S2} \\ f_I \end{bmatrix} g = \begin{bmatrix} g_{S1} \\ g_{S2} \\ g_I \end{bmatrix} \tag{2}$$

Compatibility condition (coupling equations) is expressed as

$$\boldsymbol{B}x = 0 \tag{3}$$

where $\boldsymbol{B}$ is Boolean since the interface degrees of freedom match. And the coupling equations are very simple $x^{(k)} - x^{(l)} = 0$. Equilibrium condition is given by

$$\boldsymbol{L}^T g = 0, \tag{4}$$

where $\boldsymbol{L}$ is Boolean matrix describing the relations among the interface forces. $\boldsymbol{L}$ is null space of $\boldsymbol{B}$.

The matrices of coupled system $\widetilde{\boldsymbol{M}}, \widetilde{\boldsymbol{C}}, \widetilde{\boldsymbol{K}}$ and vector $\tilde{f}$ are expressed as

$$\begin{aligned} \widetilde{\boldsymbol{M}} &\triangleq \boldsymbol{L}^T \boldsymbol{M} \boldsymbol{L} \\ \widetilde{\boldsymbol{C}} &\triangleq \boldsymbol{L}^T \boldsymbol{C} \boldsymbol{L} \\ \widetilde{\boldsymbol{K}} &\triangleq \boldsymbol{L}^T \boldsymbol{K} \boldsymbol{L} \\ \tilde{f} &\triangleq \boldsymbol{L}^T f \end{aligned} \tag{5}$$

The next step in the identification is comparison of FRFs of the coupled model and FRFs measured on the real bolted assembly. The correlation coefficient ( 6 ) can be used to describe agreement between calculated FRFs and FRFs measured on bolted specimens.

$$R = \frac{\sum_{i=1}^{N}(X_i - \bar{X})(Y_i - \bar{Y})}{\sqrt{\sum_{i=1}^{N}(X_i - \bar{X})^2}\sqrt{\sum_{i=1}^{N}(Y_i - \bar{Y})^2}} \tag{6}$$

Value of the correlation coefficient can be then used as objective function for a genetic algorithm, which finds the best $\boldsymbol{M_I}, \boldsymbol{C_I}, \boldsymbol{K_I}$ matrices.

Compared to using the, $\boldsymbol{C}$, $\boldsymbol{K}$ matrices, receptance matrix (Fig. 1), representation of the joint properties features some advantages since the FE model identification can introduce additional errors to the interface identification process. Another advantage is elimination of the local deformations in the FE model nodes connected to spring damper elements

introduced in [2]. This allows for reduction in the number of interface nodes and could also lead to reduction of unknown parameters in the identification.

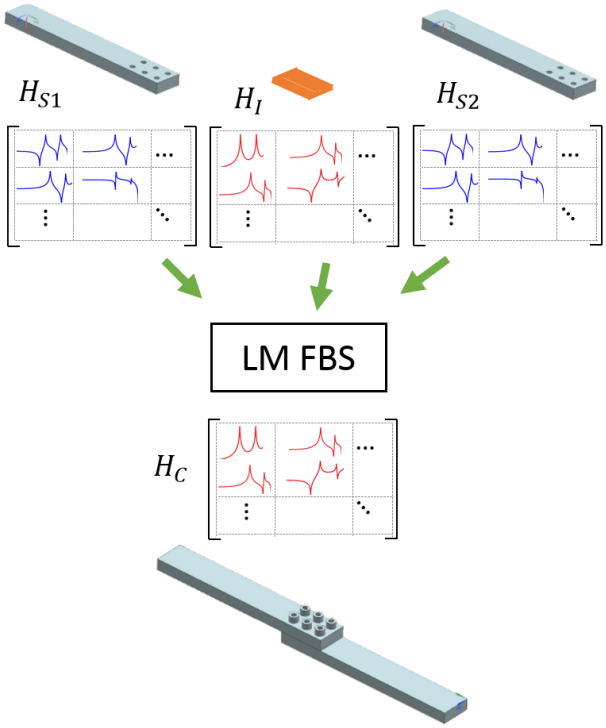


Fig. 1. Coupling of receptance matrices $H_{S1}$ and $H_{S2}$ of two parts and the interface receptance matrix $H_I$ by LM FBS method to get receptance matrix of the assembly

If the receptance matrices are used, is the receptance matrix of the interface $\boldsymbol{H_I}$ calculated from the $\boldsymbol{M_I}$, $\boldsymbol{C_I}$, $\boldsymbol{K_I}$ matrices (Fig. 2). The measured matrices $\boldsymbol{H_{Si}}$ and the interface matrix $\boldsymbol{H_I}$ are then coupled using Lagrange Multiplier Frequency Based Substructuring Method (LM FBS) [4]. It is actually the same coupling approach as described above, but in frequency domain.

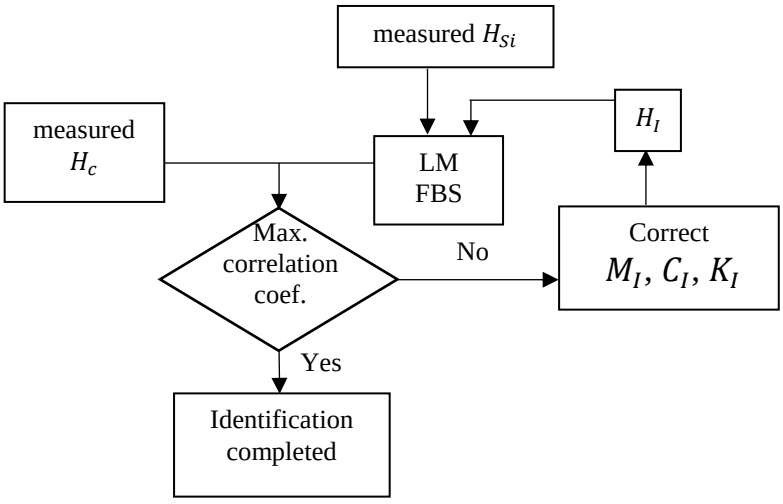


Fig. 2. Identification of joint properties

## 3. COUPLING USING RECEPTANCE MATRIX REPRESENTATION

The key component of the interface identification method presented in the previous chapter is model coupling. A study of receptence matrix coupling of a beam specimen was conducted to investigate accuracy of the receptance matrix representation and the coupling method. While coupling the receptance matrices can eliminate errors during FE model identification and less interface nodes are necessary, there are some additional problems involved in this approach. The most important one is the need to measure many more frequency response functions (FRF). In the case of six interface nodes Fig. 3 altogether 441 FRFs are needed (6 nodes in the interface, 1 node to check the resulting FRF, 3 DOFs at each node ~ (7*3)^2 =441. Another problem is that some of these FRFs cannot be actually measured. It is obvious that point 4 for example cannot be hit in *x* direction when using a modal hammer to excite the specimen. The aim of this section is to investigate, which FRFs are really necessary, which could be omitted and what effect would omitting them have on the results.

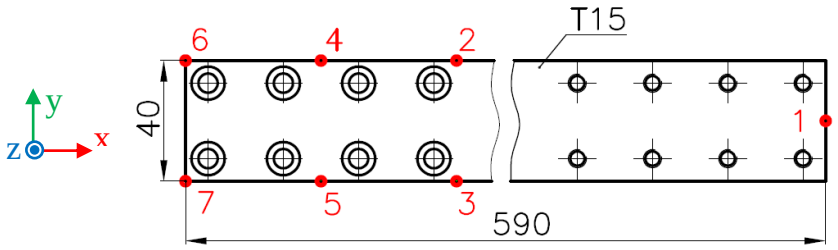


Fig. 3. Dimensions and coupling points of specimen A, material steel

The study of the influence of FRFs in the single specimen receptance matrix $\boldsymbol{H_S}$ on the FRFs in matrix $\boldsymbol{H_C}$ coupled by LM FBS method was done with data obtained from a FEM model. The specimen A was coupled to another specimen A, at six nodes shown in Fig. 3. So the receptance matrices $\boldsymbol{H_{S1}}$ and $\boldsymbol{H_{S2}}$ are the same.

The calculated $\boldsymbol{H_{Si}}$ matrices are coupled directly together without any interface model (same principle as shown in Fig. 2, just the interface is missing). The coupled models are compared to FE model of the assembly in which are the interface nodes simply merged, so there is no interface influence either (number of merged nodes is much higher than six to eliminate influence of the local stiffness around them). All FRFs were created using modal synthesys with no damping, because damping ratio inserted to model before coupling would result in different unknown damping ratio of the coupled model. The simplifications mentioned above allow to asses influence of particular FRFs in the $\boldsymbol{H_{Si}}$ matrices on the FRFs in the $\boldsymbol{H_C}$ matrix with minimum of other influences.

Fig. 4 shows effect of the first simplification of the $\boldsymbol{H_{Si}}$ matrices on coupled FRF in *z* direction which is neglecting the *x* degree of freedom. It can be seen that the red curve corresponding to model coupled in all three degrees of freedom fits very well the FE coupled model (blue curve). Neglecting the *x* degree of freedom (green curve) means that the properties in this direction cannot be identified directly and the results in the remaining two directions are influenced too.

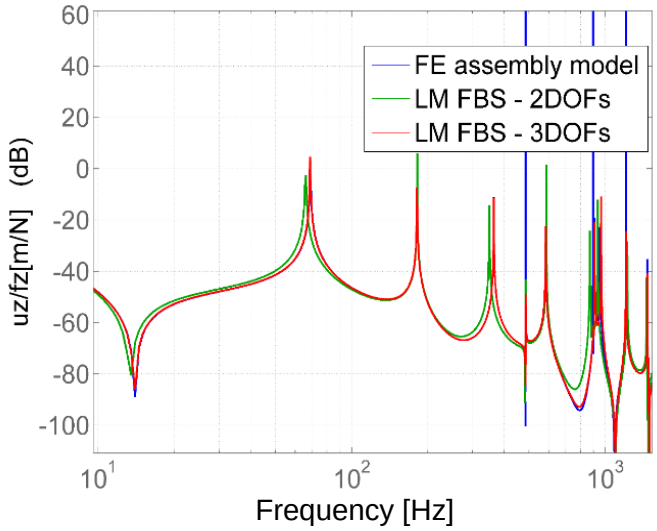


Fig. 4. FRF uz1/Fz1 calculated from the FE assembly, models coupled by LM FBS in two degrees of freedom and in three degrees of freedom

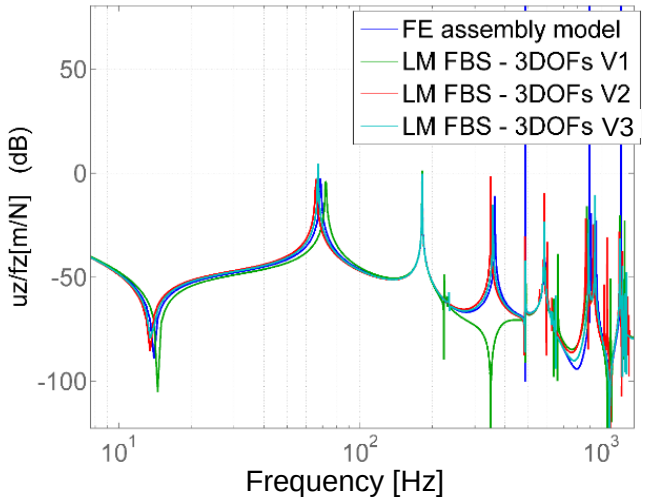


Fig. 5. FRF uz1/ Fz1 calculated from the FE assembly, and three models coupled by LM FBS with simplified receptance matrices

Another option could be to replace some of the unmeasurable FRFs with other FRFs and set the rest to zeros. The FRFs ux/Fx can only be measured at points 1, 6 and 7. In the V1 variant of the $\boldsymbol{H_{Si}}$ matrices Fig. were the unmeasurable diagonal FRFs at points 2, 3, 4 and 5 simply replaced with FRFs measured at points 6 and 7, the rest was set to zero for all frequencies. It can be seen that this gives even worse results than simple omitting the *x* direction Fig. 5.

In the V2 variant of the $\boldsymbol{H_{Si}}$ matrices Fig. 7 were the unmeasurable diagonal FRFs replaced the same way as in the V1 variant. Because the response matrix is symmetric (in theory least) most of the non-diagonal FRFs are substituted with their symmetric equivalents (ux1/ Fx5 = ux5/Fx1).

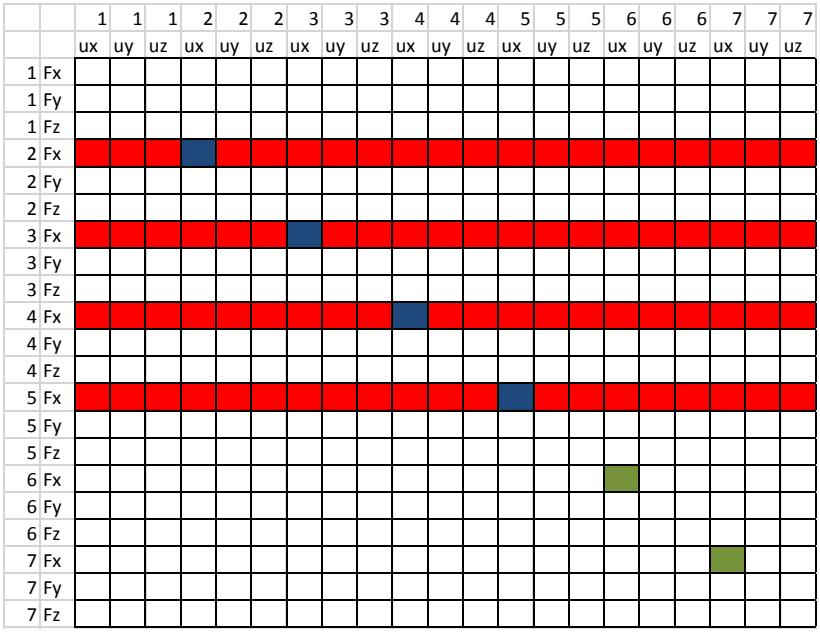


Fig. 6. Receptance matrix V1, ■ - set to zeros, ■ - copied from node 6 and 7 ■

Those without a symmetric equivalent were set to zero (for example ux5/Fx4 and ux4/Fx5 are both unknown). V2 gives better agreement with the reference FEM model than V1, but not better than omitting the *x* direction and connecting the two receptance matrices just in two degrees of freedom. Problematic are especially new peaks occurring at higher frequencies.

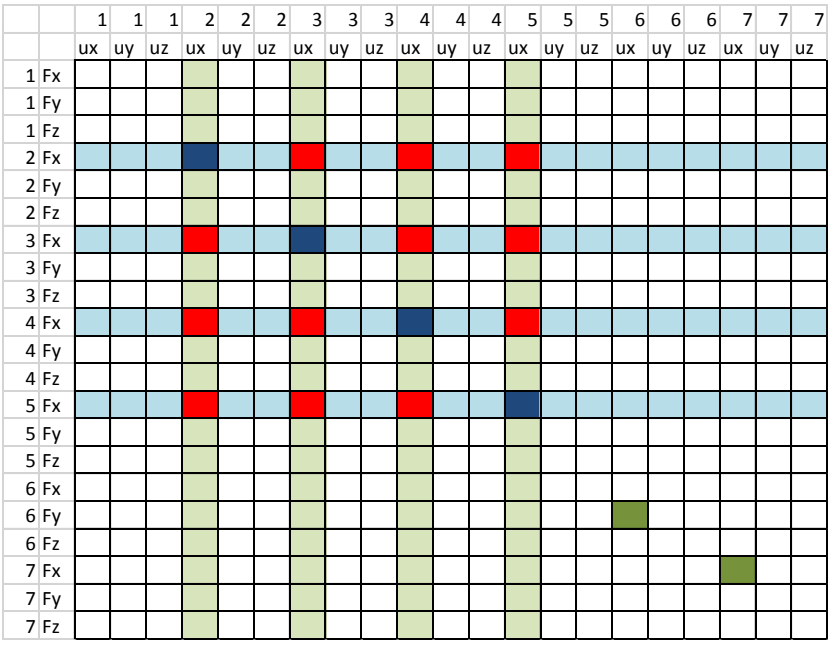


Fig. 7. Receptance matrix V2, ■ - set to zeros, ■ - copied from node 6 and 7 ■, ■ - copied from corresponding columns ■

Another option is tested in the variant V3, which is the same as V2 except the unknown non-diagonal FRFs were not set to zero. They were substituted with FRFs measured at points 6 and 7 Fig. 8. The results are more or less the same as the results of V2.

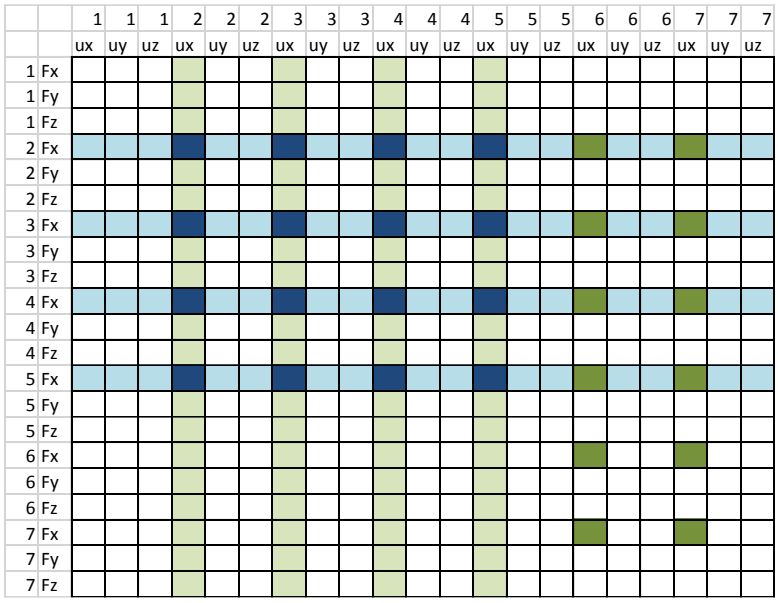


Fig. 8. Receptance matrix V3, - set to zeros, - copied from node 6 and 7, - copied from corresponding columns

Computational tests performed reveal, that copying the receptance matrix diagonal elements is not sufficient (V1) and using the non-diagonal elements, taking at the same time the advantage of their symmetry (V2, V3) is needed. However, it can be seen on the other hand that coupling using just the *y* and *z* directions provide also sufficiently precise results.

### 3.1. COUPLING THE MEASURED RECEPTANCE MATRICES

Response functions were measured on the part A used for theoretical analysis in the previous section (Fig. 3) and on part B (Fig. 9) which represents ideally joined bodies (A + A). The FRFs were measured in four points on the interface (2, 3, 6 and 7) and in the reference point 1. Lower number of interfacing points is justified by the purpose of the experiment which is to find out whether it is possible to get FRFs comparable to the ones measured on part B.

Comparison of the FRF between the points 101 and 201 in the z direction measured on the part B and the FRF resulting from coupling the measured receptance matrices of the A part by the LM FBS method is show in Fig. 10.

It can be seen that the coupled FRF is significantly affected by noise. It seems that the noise was actually magnified by the coupling method because the original FRFs were relatively smooth. Noisy were only the FRFs between different directions (uy/Fz, uz/Fy)

which should have less influence on resulting FRF than the ones between the same directions.

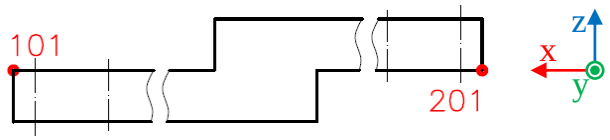


Fig. 9. Reference points of specimen B, single piece of steel in the shape of two assembled specimens A

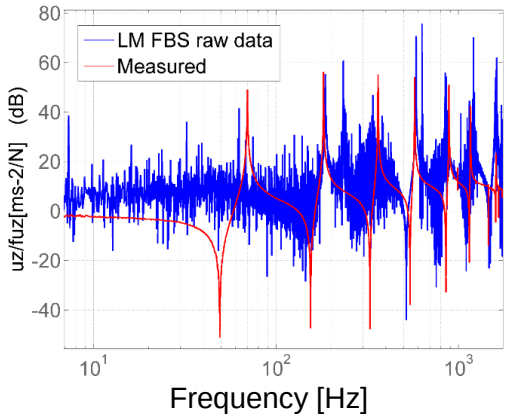


Fig. 10. uz101/Fz101 measured on part B and calculated by FM FBS using receptance matrices measured on part A

The FRFs in the receptance matrices $\boldsymbol{H_{Si}}$ were smoothed by combination of signal filtering and system identification techniques to minimize the noise influence (Fig. 11) (Fig. 12). The comparison of the coupled and measured FRFs after smoothing the original FRFs is shown in Fig. 13. It can be seen that some resonance and anti-resonance peaks coincide with the measurement on the specimen B, while most of them don't.

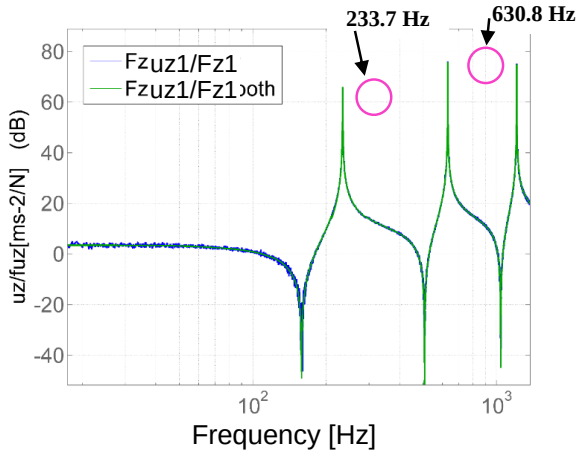


Fig. 11. uz1/Fz1 measured on specimen A (raw data) and smoothed

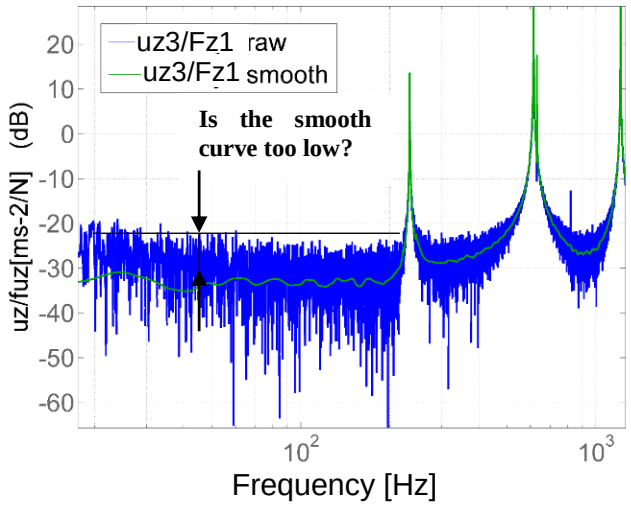


Fig. 12. uy3/Fz1 measured on specimen A (raw data) and smoothed

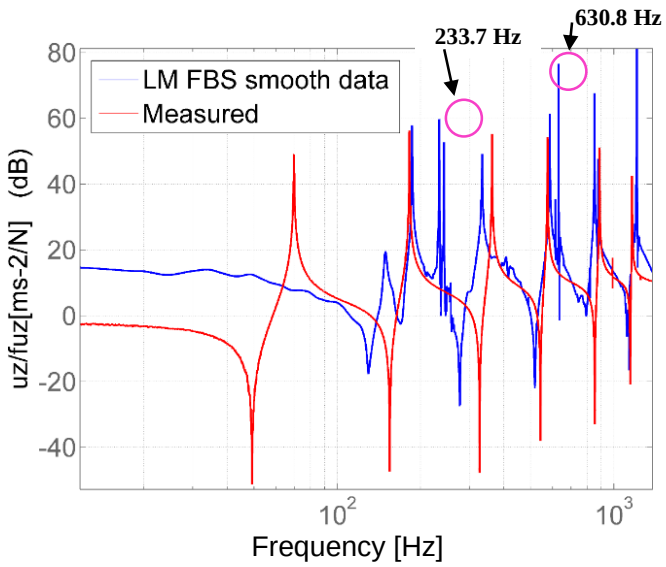


Fig. 13. uz101/Fz101 measured on part B and calculated by FM FBS from smoothed receptance matrices measured on part A

Significant mismatch in the area up to the second resonance peak results probably from an insufficient smoothing and possible errors in the values of the smoothed FRF. The problem is probably caused by the FRFs between different directions (Fig. 12) which contain a lot more noise than those between the same directions (Fig. 11). High level of noise in these FRFs can always be expected because accelerometers are a lot less excited when impact of the modal hammer does not occur in its measuring direction.

Another interesting thing is the presence of resonance peaks of the part A in the coupled FRF at cca 234Hz and 631Hz. The peaks are well preserved in the filtered FRFs of the single part (Fig. 11) but they didn't cancel out after coupling (Fig. 13). The peaks are quite narrow so their presence may results from errors in the measured peak height.

## 4. COUPLING USING FE MODELS

The results in the previous section have shown that use of the FRFs directly measured using part A and coupling those FRFs to get the coupled system FRF gives not fully reliable results. An alternative approach is to use FE models as a representation of the bodies to be coupled and fit them to the measured FRFs.

Values of the resonance frequencies can relatively easily be matched by modifying the Young's modulus and density of the FE model's material. Match of the dynamic compliances is more difficult to achieve because it is related to damping. The first additional source of errors is the method used for damping ratios identification (using peak pick, circle fit, or any other method). The identified damping ratios can be used to estimate mass and stiffness proportional damping coefficients assuming Rayleigh damping model. Even if the damping is proportional it is unlikely that it will be perfectly described by just the two damping coefficients, hence more errors in the peak heights.

An advantage of FE model fitting is the possibility to use the $\boldsymbol{M_I}$, $\boldsymbol{C_I}$, $\boldsymbol{K_I}$ matrices in model coupling and availability of all FRFs in the $H$ matrix if the FRF based model coupling is to be used.

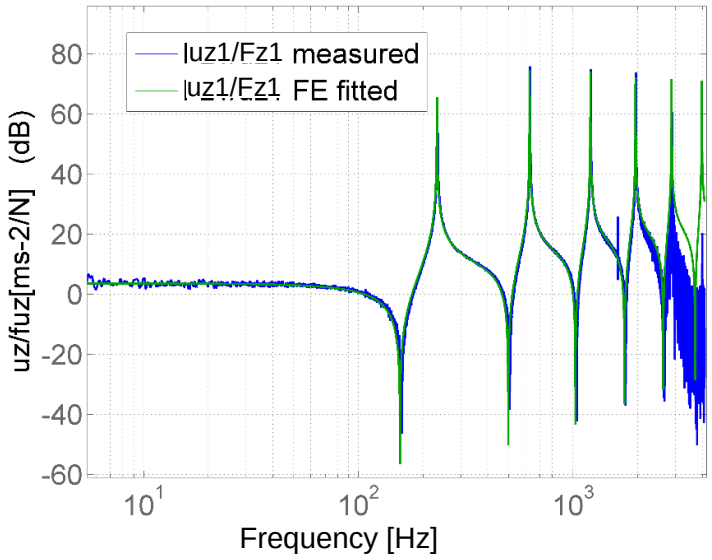


Fig. 14. FRF uz1/Fz1 measured on one part and the same FRF of a fitted reference FE model

The FRF uz1/Fz1 measured on part A and the same FRF of the fitted model is shown in Fig. 14. It can be seen that the fit is relatively good in this case. The coupled fitted models are compared to the data measured on specimen B in Fig. 15. There are some differences in the peak heights, which are increasing with the frequency. This is probably caused by measurement errors. Slight deviations in the resonance frequencies may also be seen even if the part A fitted single FE model has matched the measured FRF very well.

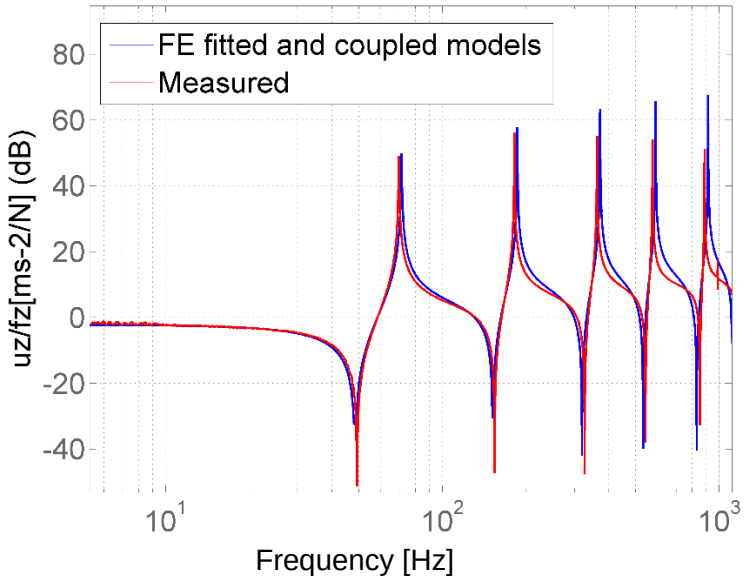


Fig. 15. FRF uz101/Fz101 measured on specimen B and calculated from fitted and coupled FE models

## 5. CONCLUSION

An approach of bolted joint identification is proposed considering the joint representation by either the full mass, stiffness and damping matrices or by the receptance matrix. Main prerequisite for relevant identification of the joint properties is represented by using a reliable method for describing the dynamic properties of the parts to be coupled. The study presented in the paper focuses on two methods – representation of the part properties by mass, stiffness and damping matrices, or by receptance matrices using a case of two beams coupling. Both approaches are suited for joint properties identification, as proposed in the paper.

Receptance matrix representation gives an advantage that the frequency response functions measured can directly be used for mathematical coupling and consequent identification of the joint properties. However, significant difficulties are detected disallowing for a reliable application of this approach. First, many FRF measurements needs to be performed and second, measurement noise considerably affects the accuracy of the coupled FRFs. Contrary to this, an approach based on using the fitted FE models of the coupled parts to calculate the coupled system FRFs provides very good results both in terms of eigenfrequencies and dynamic compliances.

ACKNOWLEDGEMENT

*This research has been supported by the Competence Center - Manufacturing Technology project TE01020075 funded by the Technology Agency of the Czech Republic. This work was supported by the Grant Agency of the Czech Technical University in Prague, grant No. SGS13/190/OHK2/3T/12.*

REFERENCES

[1] ITO Y., 2008, *Modular design for machine tools*, McGraw-Hill.
[2] SHIMIZU S., Kabaya Y., Sakamoto H, Kenichi Yamashita K., 2013, *Identification Method of Dynamic Characteristics of Joints in Jointed Structures*, International Journal of Automation Technology, **7**/7, 221−227.
[3] DE KLERK D., RIXEN D., VOORMEEREN S., 2008, *General framework for dynamic substructuring: History, review, and classification of techniques*, AIAA Journal, 46/5, 1169−1181.
[4] DE KLERK D., RIXEN D.J., DE JONG J., 2006, *The Frequency Based Substructuring (FBS) Method reformulated according to the Dual Domain, In: Proceedings of the 15th International Modal Analysis* Conference, Society of experimental machanics, 136.